Supporting information for:

Visual extrapolation of contour geometry

Manish Singh and Jacqueline M. Fulvio

Proceedings of the National Academy of Sciences, 102 (3), 939-944.

Supporting Information: Figure 6

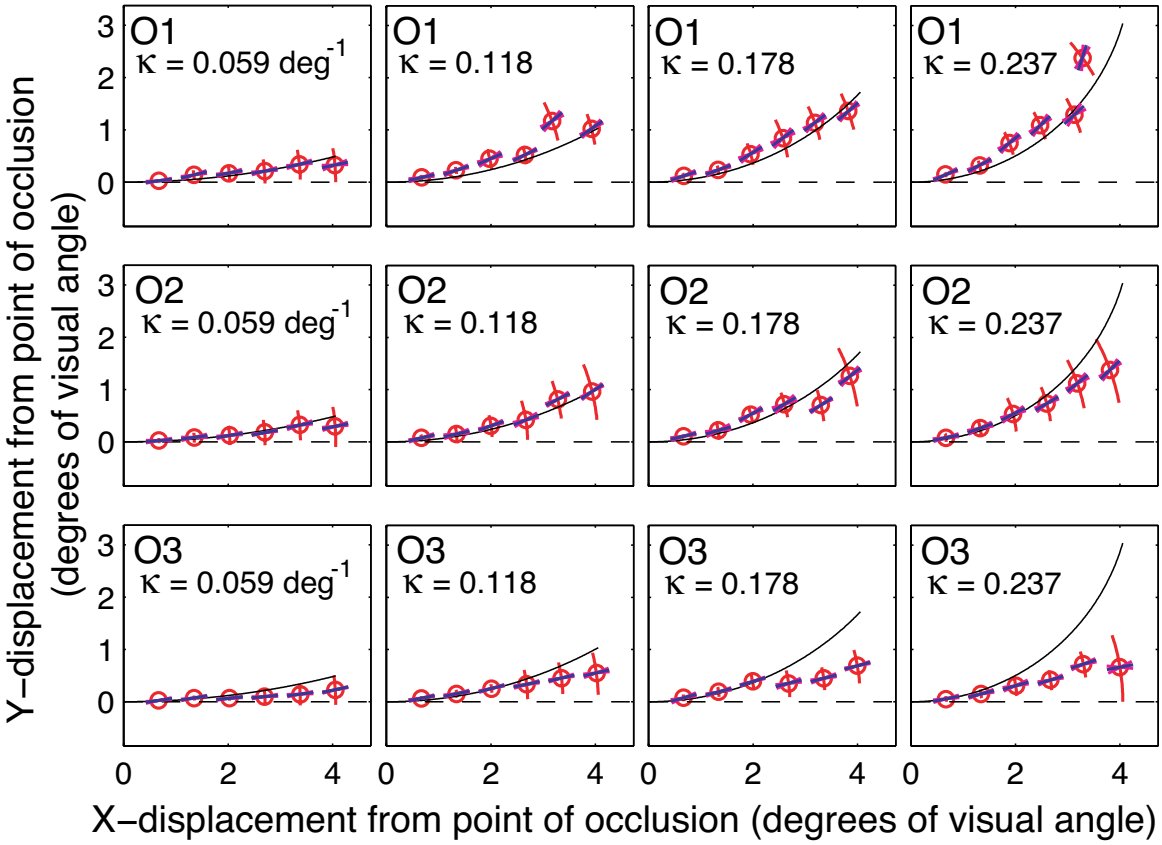

Figure 6. Extrapolation data for the circular-arc inducers. The mean settings of angular position and orientation are shown in the Cartesian plane, at each of the six radial distances, with standard-deviation bars for angular position and standard-deviation cones for orientation. The solid curves show the actual extensions of the circular arcs used to define the inducers. The dashed lines correspond to the linear extensions of the inducer tangents at the point of occlusion.

Supporting Information: Figure 7

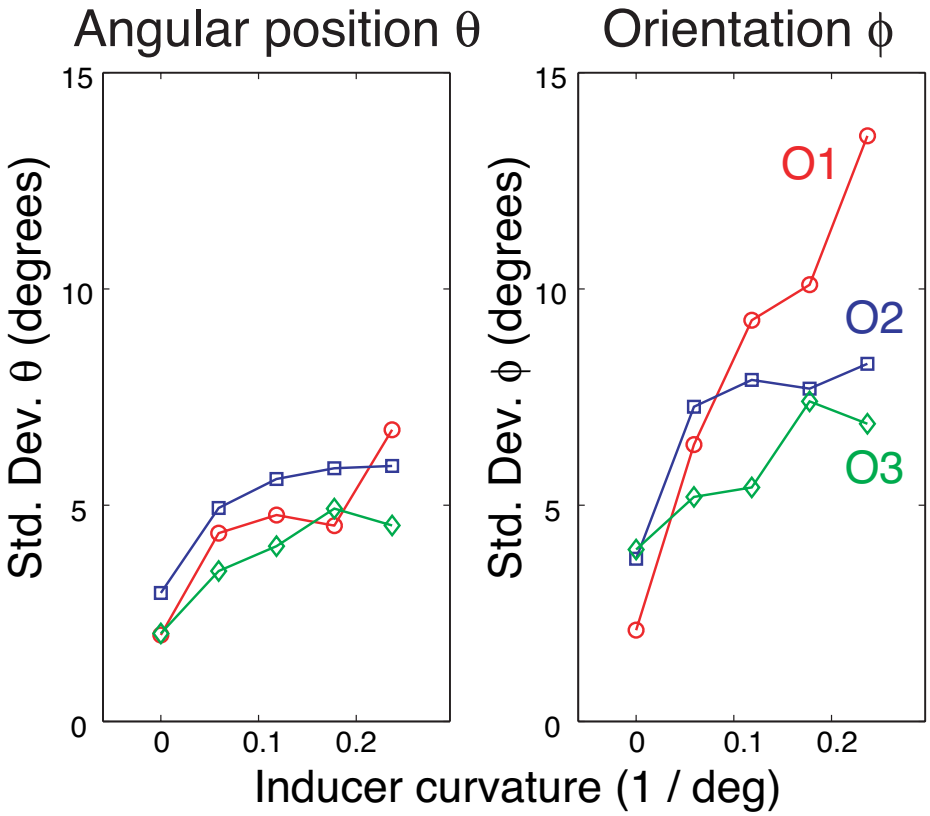

Figure 7. Standard deviations in probe position and orientation plotted as a function of the curvature of the parabolic inducers. Tests of heteroscedasticity revealed a significant dependence of setting variability on inducer curvature in all 6 cases. This demonstrates a *cost of curvature*—i.e., a systematic decline in the overall precision with which angular position and orientation are represented, with increasing inducer curvature.

Supporting Information: Table 1

Bayes Factors for the parabolic model $\mathcal{M}_p$ against the circular model $\mathcal{M}_c$

Inducer	Parabolic inducers			Circular inducers		
Curvature	O1	O2	O3	O1	O2	O3
0.059	1.094	1.012	1.184	1.20	1.012	1.052
0.118	5.73	4.41	1.93	60.48	2.53	5.38
0.178	$>10^2$	7.58	6.69	$>10^3$	57.85	16.23
0.237	1.43	$>10^2$	6.94	24.16	15.77	6.35

Table 1. Values of Bayes factors for the parabolic model $\mathcal{M}_p$ against the circular model $\mathcal{M}_c$. All values are greater than 1, indicating that the parabolic model provides a consistently better fit to the extrapolation data than the circular model—irrespective of whether the inducers themselves are parabolic or circular.

Supporting Information: Figure 8

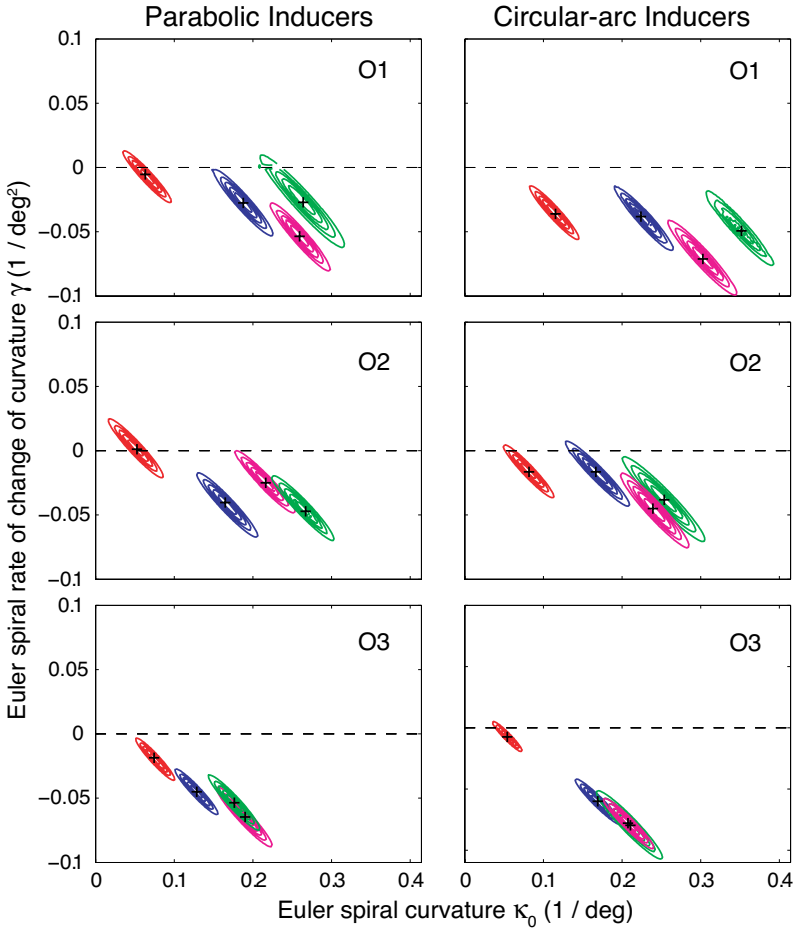

Figure 8. Contour plots of the standardized likelihood surfaces for the fits of the Euler-spiral model to the extrapolation data. The four surfaces in each plot correspond to the four different inducer curvatures. The maximum-likelihood estimates of the parameters (κ, γ) are marked with '+' symbols. 23 of the 24 cases yield negative estimates for γ, thereby indicating decreasing curvature along extrapolated contours. (See also the statistical tests reported in Supporting Table 2.)

Supporting Information: Table 2

Log likelihood-ratio statistic Δ for the Euler-spiral model $\mathcal{M}_{es}$ against the circular-arc model $\mathcal{M}_c$

Inducer	Parabolic inducers			Circular inducers		
Curvature	O1	O2	O3	O1	O2	O3
0.059	0.500	0.154	5.375*	10.195*	2.164	1.459
0.118	3.999*	10.238*	23.158*	9.586*	1.890	38.500*
0.178	15.529*	3.934*	27.877*	21.316*	9.610*	52.157*
0.237	1.881	11.383*	22.225*	9.673*	4.751*	28.999*

Table 2. Values of the log likelihood-ratio statistic for the Euler-spiral model $\mathcal{M}_{es}$ against the circular model $\mathcal{M}_c$ (i.e., degenerate case of the Euler-spiral model with $\gamma = 0$). This statistic is given by twice the log of the ratio of the maximized likelihood values under the two models, i.e., $\Delta = 2\log(L_{es}/L_c)$, where $L_c = \max_\kappa \ell_c(\kappa|\mathcal{D})$ and $L_{es} = \max_{(\kappa,\gamma)} \ell_{es}((\kappa,\gamma)|\mathcal{D})$. Because $\mathcal{M}_c$ is nested within $\mathcal{M}_{es}$, the ratio of the likelihoods cannot be smaller than 1 (and therefore the statistic Δ cannot be negative). In order to set a cut-off value, we use the fact that, under the null hypothesis that model $\mathcal{M}_c$ is corrrect, Δ is asymptotically distributed as a χ^2 with 1 degree of freedom (= the difference in the number of parameters between the two models). Cases where the null hypothesis of the circular model is rejected at the $.05$ level—and thus the γ estimate is significantly different than 0—are marked with asterisks.

Supporting Information: Table 3

Bayes Factors for the log-spiral model $\mathcal{M}_{ls}$ against the Euler-spiral model $\mathcal{M}_{es}$

Inducer	Parabolic inducers			Circular inducers		
Curvature	O1	O2	O3	O1	O2	O3
0.059	28.41	18.54	$>10^2$	$>10^2$	61.27	$>10^2$
0.118	16.85	$>10^2$	$>10^3$	26.45	8.95	$>10^3$
0.178	2.42	5.45	$>10^4$	$>10^2$	68.36	$>10^3$
0.237	10.50	28.90	$>10^4$	67.26	12.74	34.14

Table 3. Values of Bayes factors (= posterior odds) for the logarithmic-spiral model $\mathcal{M}_{ls}$ against the Euler-spiral model $\mathcal{M}_{es}$, for the extrapolation data with parabolic and circular inducers. All values are greater than 1, indicating that the log-spiral model consistently provides a better fit to the extrapolation data, than the Euler-spiral model.

Supporting Information:
Derivation of the general Cartesian form of the logarithmic spiral

The logarithmic spiral is standardly expressed in polar coordinates as:

$$r = \alpha e^{\beta\theta}$$

However, this form is not useful for our purposes because it describes a log spiral whose pole (point of infinite curvature) is at the origin. We require a form that is general enough to describe a spiral "starting" at an arbitrary initial position (x_0, y_0), with initial tangent direction ϕ_0, initial curvature κ_0, and initial rate of change of curvature γ_0 at that point. We derive such a form in the complex Cartesian plane.

We begin with the following Cesàro equation, expressing curvature in terms of arc length:

$$\kappa(s) = \frac{1}{bs + a}$$

The values a and b are chosen to ensure that the initial curvature and rate of curvature are κ_0 and γ_0, respectively. Specifically:

$$a = \frac{1}{\kappa_0} \qquad \text{and} \qquad b = -\frac{\gamma_0}{\kappa_0^2}$$

The orientation function is then given by:

$$\begin{aligned} \phi(s) &= \phi_0 + \int_0^s \frac{dt}{bt + a} \\ &= \phi_0 + \frac{1}{b}[\log(bs + a) - \log(a)] \end{aligned}$$

and the position $\mathcal{E}(s) = x(s) + iy(s)$ is given by:

$$\begin{aligned} \mathcal{E}(s) &= \mathcal{E}(0) + \int_0^s e^{i\left(\phi_0 + \frac{1}{b}[\log(bt+a) - \log(a)]\right)} dt \\ &= \mathcal{E}(0) + e^{i\left(\phi_0 - \frac{1}{b}\log(a)\right)} \left[\int_0^s \cos\left(\frac{\log(bt + a)}{b}\right) dt + i \int_0^s \sin\left(\frac{\log(bt + a)}{b}\right) dt \right] \\ &= \mathcal{E}(0) + e^{i\left(\phi_0 - \frac{1}{b}\log(a)\right)} [I_1 + iI_2] \end{aligned}$$

In order to obtain the general expression, we need to evaluate the two integrals I_1 and I_2. Setting $u = \log(bt + a)/b$, we obtain:

$$I_1 = \int_0^s \cos\left(\frac{\log(bt + a)}{b}\right) dt = \int_{u_1}^{u_2} e^{bu} \cos(u) du$$

where $u_1 = \frac{1}{b}log(a)$ and $u_1 = \frac{1}{b}log(bs+a)$. Using integration by parts,

$$\begin{aligned} I_1 &= e^{bu}\sin(u)\Big|_{u_1}^{u_2} - b\int_{u_1}^{u_2} e^{bu}\sin(u)du \\ &= e^{bu}\sin(u)\Big|_{u_1}^{u_2} - b\Big[-e^{bu}\cos(u)\Big|_{u_1}^{u_2} + b\int_{u_1}^{u_2} e^{bu}\cos(u)du\Big] \\ &= e^{bu}\sin(u)\Big|_{u_1}^{u_2} + be^{bu}\cos(u)\Big|_{u_1}^{u_2} - b^2 I_1 \end{aligned}$$

and therefore,

$$\begin{aligned} I_1 &= \frac{1}{1+b^2}\cdot e^{bu}[\sin(u)+b\cos(u)]\Big|_{u_1}^{u_2} \\ &= \frac{bs+a}{1+b^2}\Big[\sin\Big(\frac{\log(bs+a)}{b}\Big)+b\cos\Big(\frac{\log(bs+a)}{b}\Big)\Big] - \frac{a}{1+b^2}\Big[\sin\Big(\frac{\log a}{b}\Big)+b\cos\Big(\frac{\log a}{b}\Big)\Big] \end{aligned}$$

Similarly,

$$I_2 = \int_0^s \sin\big(\frac{\log(bt+a)}{b}\big)dt = \int_{u_1}^{u_2} e^{bu}\sin(u)du$$

where $u_1 = \frac{1}{b}log(a)$ and $u_1 = \frac{1}{b}log(bs+a)$. Using integration by parts as before,

$$\begin{aligned} I_2 &= -e^{bu}\cos(u)\Big|_{u_1}^{u_2} + b\int_{u_1}^{u_2} e^{bu}\cos(u)du \\ &= -e^{bu}\cos(u)\Big|_{u_1}^{u_2} + b\Big[e^{bu}\sin(u)\Big|_{u_1}^{u_2} - b\int_{u_1}^{u_2} e^{bu}\sin(u)du\Big] \\ &= -e^{bu}\cos(u)\Big|_{u_1}^{u_2} + be^{bu}\sin(u)\Big|_{u_1}^{u_2} - b^2 I_2 \end{aligned}$$

and therefore,

$$\begin{aligned} I_2 &= \frac{1}{1+b^2}\cdot e^{bu}[b\sin(u)-\cos(u)]\Big|_{u_1}^{u_2} \\ &= \frac{bs+a}{1+b^2}\Big[b\sin\Big(\frac{\log(bs+a)}{b}\Big)-\cos\Big(\frac{\log(bs+a)}{b}\Big)\Big] - \frac{a}{1+b^2}\Big[b\sin\Big(\frac{\log a}{b}\Big)-\cos\Big(\frac{\log a}{b}\Big)\Big] \end{aligned}$$

Supporting Information: Figure 9

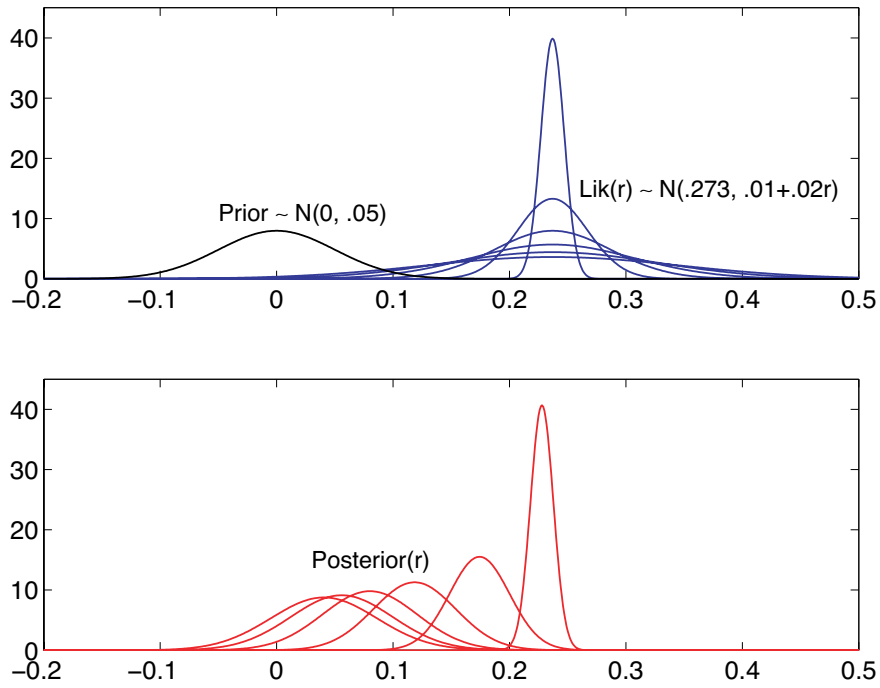

Figure 9. Demonstrating the influence of the spread of the likelihood on the Bayesian posterior. (a) Prior on curvature centered on 0, and likelihoods centered on the estimated inducer curvature. The likelihoods have increasing standard deviations (with increasing distance from the point of occlusion). (b) The posterior distributions of extrapolation curvature corresponding to the different likelihoods shown. The maximum-a-posteriori estimate of extrapolation curvature asymptotes to 0.